Properties of transient superfluids

Aditi Mitra

New York University

In collaboration with:
Dr. Yonah Lemonik (Data analyst, Moat)
Dr. Hossein Dehghani (Postdoc, JQI Maryland)
Daniel Yates

U.S. DEPARTMENT OF ENERGY | Office of Science

Quantum quench

$$|\Psi(t)\rangle = Te^{-i\int dt' H_f(t')}|\Phi_{H_i}\rangle$$

Parameters of the Hamiltonian changed in time at some arbitrary rate

Does the system thermalize to some effective temperature?

What happens when Hi is a band insulator but Hf is topological, what if
Hi supports one phase (metallic/paramagnetic/normal….) and
Hf supports another phase (insulating/magnetic/superconducting……).

THIS TALK: Initial system normal, final Hamiltonian can support superconductivity

Recent reviews:

Quantum quenches in 1+1 dimensional conformal field theories
Pasquale Calabrese, John Cardy **arXiv:1603.02889**

Quantum quench dynamics, Aditi Mitra, Annual Reviews of Condensed Matter Physics, 2018.

An optically stimulated superconducting-like phase in K_3C_{60} far above equilibrium T_c

Nature **530**, 461 (2016).

M. Mitrano[1], A. Cantaluppi[1], D. Nicoletti[1], S. Kaiser[1], A. Perucchi[2], S. Lupi[3], P. Di Pietro[2], D. Pontiroli[4], M. Riccò[4], A. Subedi[1], S. R. Clark[5,6], D. Jaksch[5,6], A. Cavalleri[1,5]

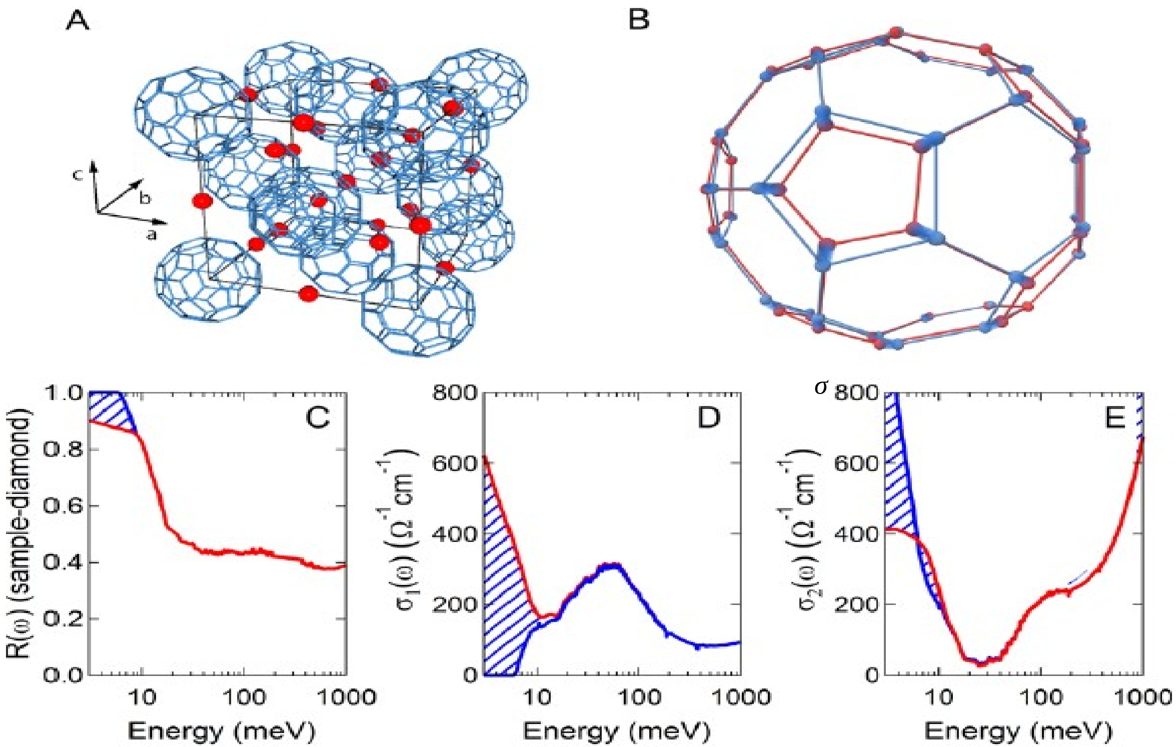

Fig. 1. Structure and equilibrium optical properties of K_3C_{60}. (A) Face centered cubic (fcc) unit cell of K_3C_{60}[xxxviii]. Blue bonds link the C atoms on each C_{60} molecule. K atoms are represented as red spheres. **(B)** C_{60} molecular distortion (red) along the $T_{1u}(4)$ vibrational mode coordinates. Equilibrium structure is displayed in blue. The displacement shown here corresponds to ~12% of the C-C bond length. **(C-E)** Equilibrium reflectivity and complex optical conductivity of K_3C_{60} measured at T = 25 K (red) and T = 10 K (blue).

Drude picture:

$$\sigma(\omega) = \frac{\sigma_0}{1 - i\omega\tau}$$

$$\sigma_0 = \frac{ne^2\tau}{m}$$

$$\mathrm{Re}\,\sigma = \frac{\sigma_0}{1+\omega^2\tau^2}$$

$$\mathrm{Im}\,\sigma = \frac{\sigma_0\omega\tau}{1+\omega^2\tau^2}$$

Nature **530**, 461 (2016).

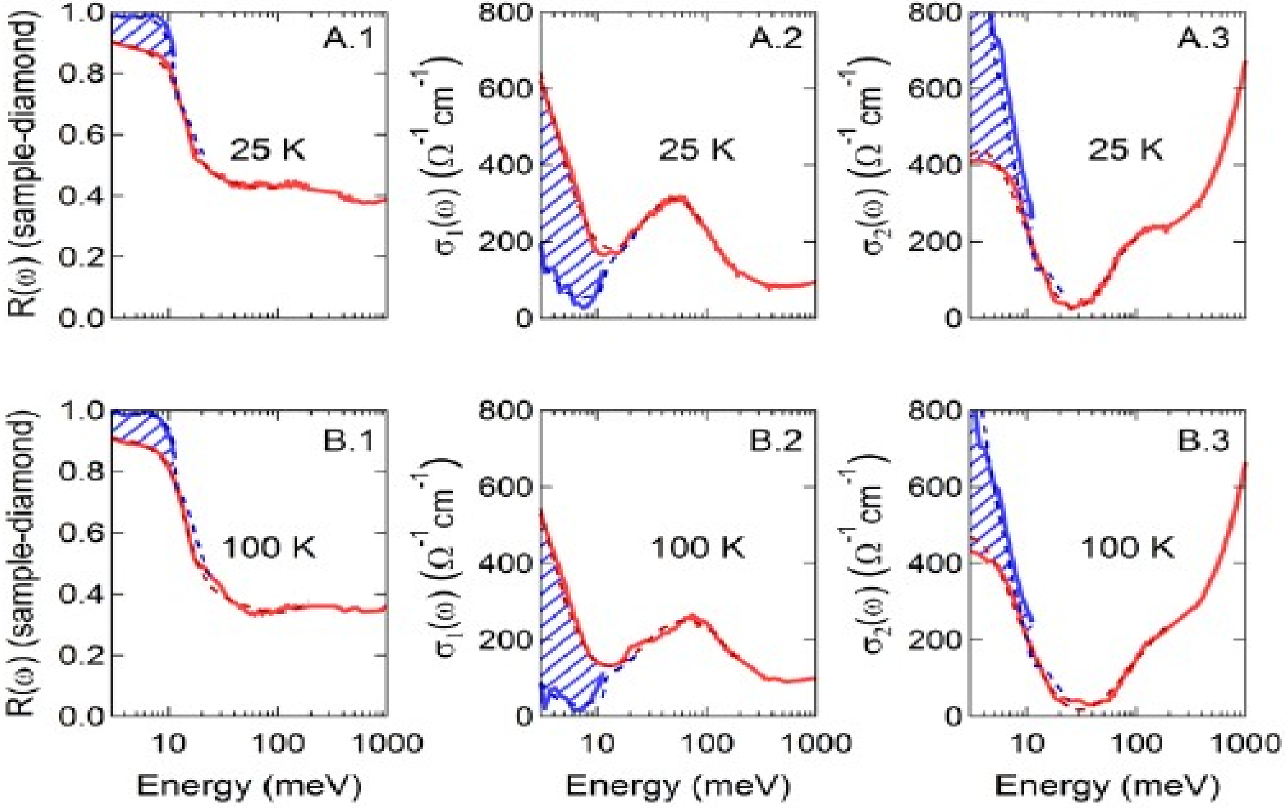

Fig. 2. Transient optical response of photo-excited K_3C_{60} at T = 25 K and T = 100 K. Reflectivity and complex optical conductivity of K_3C_{60} at equilibrium (red) and 1 ps after photo-excitation (blue) with a pump fluence of 1.1 mJ/cm², measured at base temperatures T = 25 K **(A.1-3)** and T = 100 K **(B.1-3)**. Fits to the data are displayed as dashed lines. Those at equilibrium were performed with a Drude-Lorentz model, while those for the excited state using a model describing the optical response of a superconductor with a gap of 11 meV. The band at 55 meV was assumed to stay unaffected.

State lives for 2-10 pico seconds after the initial pump

Goal 1: How can one identify the onset of superconductivity in short lived (few ps) states?

Theoretical proposals:

Pumped phonons affect the electrons by modifying the effective electron band structure/electron-phonon couplings/attractive Hubbard-U.

- Coulthard, J., Clark, S. R., Al-Assam, S., Cavalleri, A. & Jaksch, D. Enhancement of super-exchange pairing in the periodically-driven Hubbard model. *arXiv:1608.03964* (2016).
- M. Knap, M. Babadi, G. Refael, I. Martin, and E. Demler, Phys. Rev. B **94**, 214504 (2016).
- D. M. Kennes, E. Y. Wilner, D. R. Reichman, and A. J. Millis, Nature Physics **13**, 479 (2017).
- M. A. Sentef, A. Tokuno, A. Georges, and C. Kollath, Phys. Rev. Lett. **118**, 087002 (2017).
- M. A. Sentef, Phys. Rev. B **95**, 205111 (2017).

Non-superconducting scenarios:

Chiriaco, Millis, Aleiner, arxiv:1806.06645

Goal 2: Make predictions with as few material dependent fitting parameters as possible.

Outline: Transient properties of the correlated electron system

The pump acts like a "quench" where electrons are subjected to a time-dependent attractive interaction.

NO TRUE LONG RANGE ORDER, YET SUPERCONDUCTING FLUCTUATIONS ARE IMPORTANT

1.Signatures in time-resolved angle resolved photoemission tr-ARPES.

Yonah Lemonik and Aditi Mitra, *Time-resolved spectral density of interacting fermions following a quench to a superconducting critical point*, Phys. Rev. B **96**, 104506 (2017).

2. Signatures in transport such as optical conductivity for a clean system.

Yonah Lemonik and Aditi Mitra, *Transport signatures of transient superfluids*, arxiv:1711.10023
PRL in print.

3. Signatures in the optical conductivity for a disordered system.

Yonah Lemonik and Aditi Mitra, *Quench dynamics of superconducting fluctuations and optical conductivity in a disordered system*, arxiv:1804.09280

4. An example where the symmetry of the superconducting order-parameter can be controlled by "quench" amplitude.

Hossein Dehghani and Aditi Mitra, *Dynamical generation of superconducting order of different symmetries in hexagonal lattices*, Phys. Rev. B **96**, 195110 (2017).

Model (clean system)

$$H_i = \sum_{k,\sigma=\uparrow,\downarrow,\tau=1\ldots N} \epsilon\left(k + A(t)\right) c^{\dagger}_{k\sigma\tau} c_{k\sigma\tau}.$$

Effect of pumping the phonons:

$$H_f = H_i + \frac{U(t)}{N} \sum_q \Delta^{\dagger}_q \Delta_q,$$

$$\Delta_q = \sum_{k\tau} c_{k,\uparrow,\tau} c_{-k+q,\downarrow,\tau}; \; \Delta^{\dagger}_q = \sum_{k,\tau} c^{\dagger}_{-k+q,\downarrow,\tau} c^{\dagger}_{k\uparrow\tau}$$

In a superconducting phase $\langle \Delta(\vec{q} = 0) \rangle$ is non-zero

For us on the other hand $\langle \Delta(\vec{q} = 0) \rangle$ will be zero. However fluctuations in this quantity will be large.

Fluctuations measured by: $F(q) = \langle |\Delta(q,t)|^2 \rangle$

Superconducting Fluctuations in Equilibrium

$$\Delta \equiv \phi$$

$r \propto U - U_c(T)$

r: detuning from critical point

$$H_f = \int d^d x \left[\frac{1}{2}\Pi^2 + \frac{1}{2}(\nabla\phi)^2 + \frac{1}{2} r\phi^2 + \frac{u}{4!N}\phi^4 \right]$$

$$[\Pi, \phi] = i$$

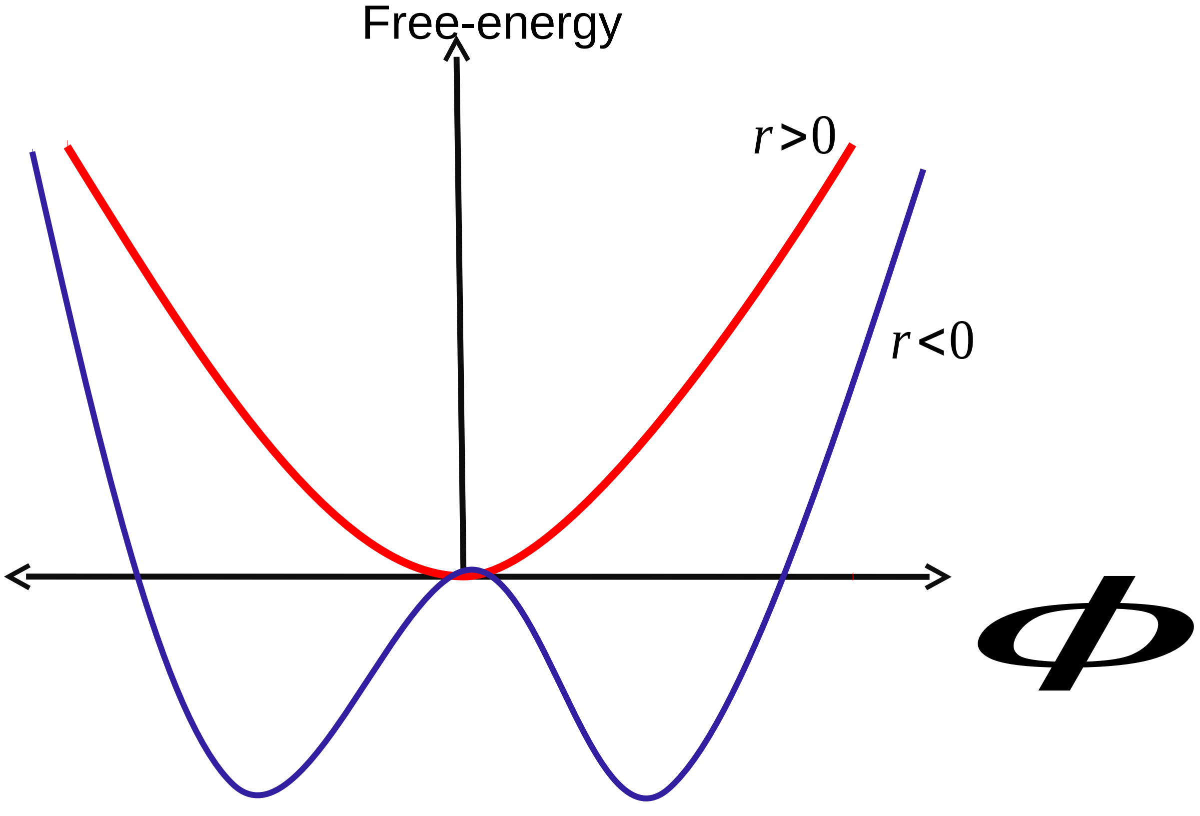

$$F_{\text{eq}}(q) = \frac{T}{v^2|q|^2/T + r}; \quad \begin{matrix} r \propto U - U_c(T) \\ vq \ll T, \quad r \ll T, \end{matrix}$$

Universal power-laws at critical point (r=0)

Fluctuations of the order-parameter at two different positions and time are strongly correlated in that they show power-law correlations:

$$\langle \phi(xt)\phi(x't) \rangle \approx \frac{1}{|x-x'|^{-2+d+\eta}}$$

$$\langle \phi(xt)\phi(xt') \rangle \approx \frac{1}{|t-t'|^{(-2+d+\eta)/z}}$$

Halperin & Hohenberg, Theory of dynamic critical phenomena, Rev. Mod. Phys. 1977

2PI action

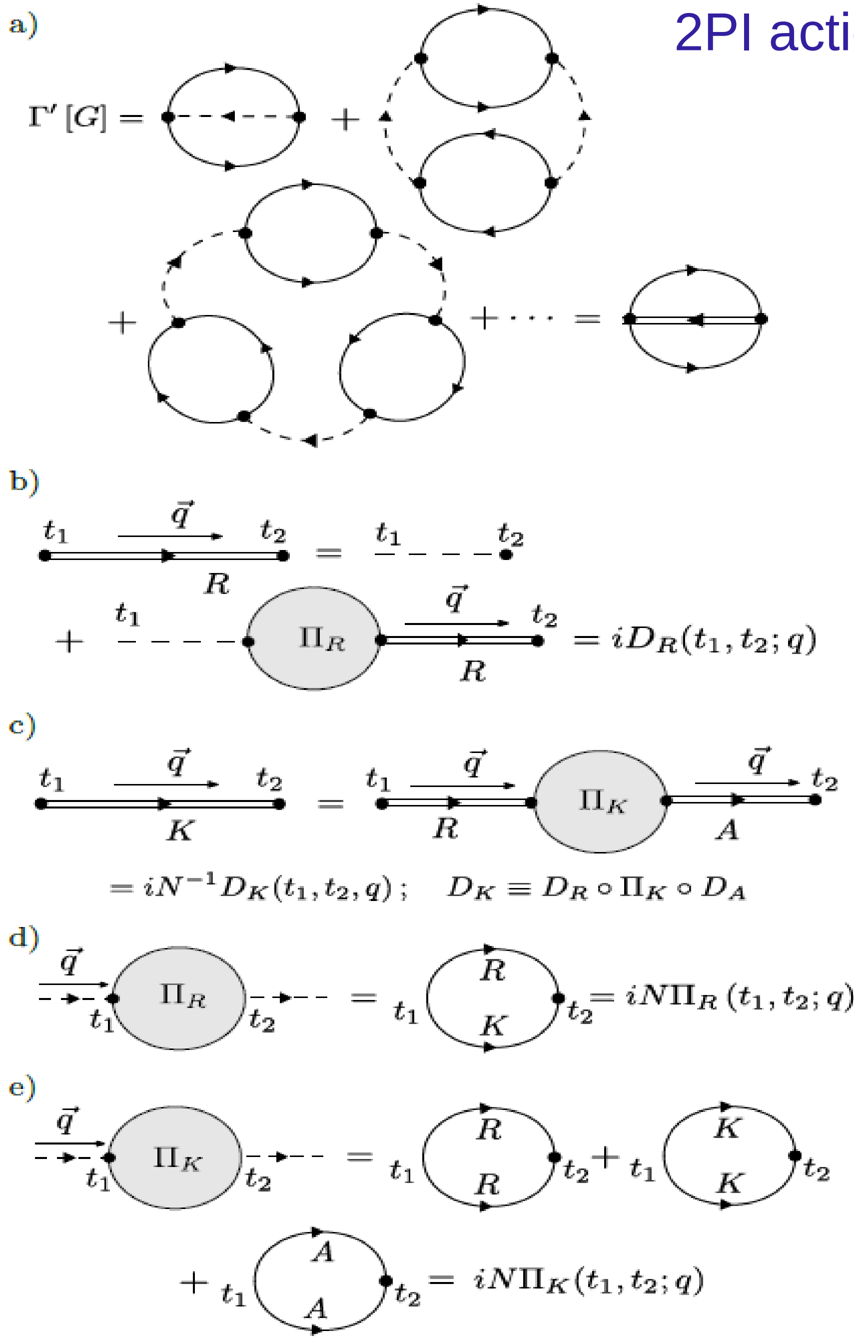

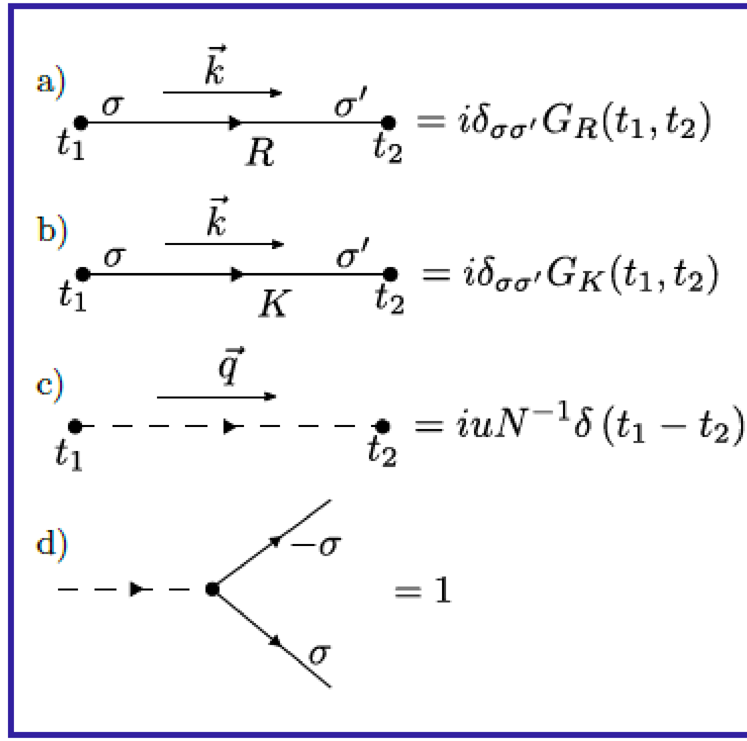

$$\Sigma_R[G] \equiv \delta\Gamma'/\delta G_A,$$

$$G_R{}^{-1} = g_R{}^{-1} - \Sigma_R[G],$$

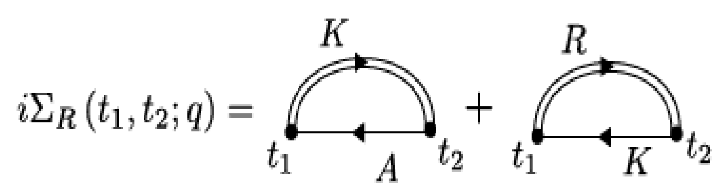

Thermalizing system

Significant simplification possible by exploiting a separation of time scales: Fermi Energy >> Temperature >> r (distance from critical point)

The dynamics for the fluctuations are,

$$\left(\partial_t + 2r(t) + 2\frac{v^2|q|^2}{T}\right) F(q,t) = T$$

Absence of higher order terms in F is due to a non-equilibrium version of the Ginzburg-Levanyuk criterion:

$$F(q=0,t) \ll E_F/T$$

In equilibrium, this criterion is:

$$r \gg T^2/E_F$$

Thus even if r(t>0)=0, the post quench transient dynamics could obey the Ginzburg-Levanyuk criterion.

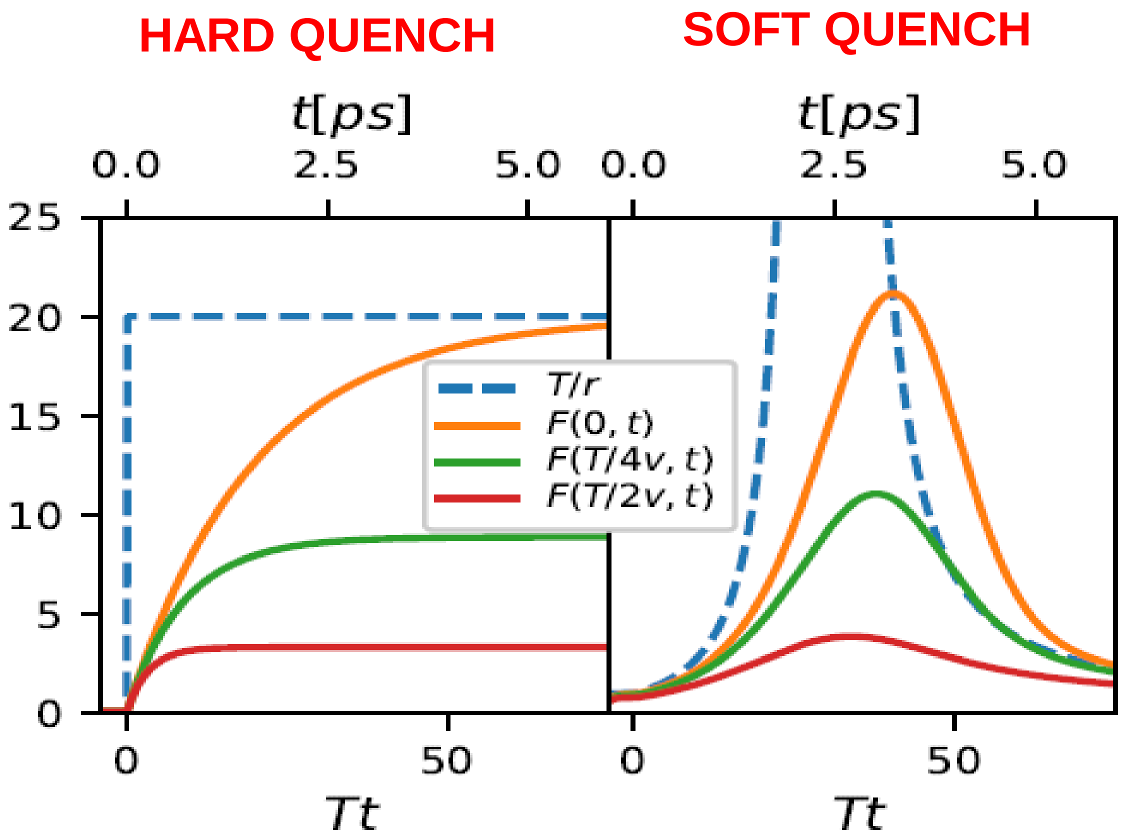

100K=1/80fs
=8.6meV

FIG. 1. Growth of superfluid fluctuations $F(q,t)$ following an interaction quench. Fluctuations at several different momenta q are shown. The times are measured in units of T^{-1} (lower axis) and in terms of ps (upper axis) for $T \sim 100$K. The quantity T/r is the inverse of the detuning from the critical point, which at equilibrium is equal to $F(q=0)$. Left: hard quench from the normal state to $T/r = 20$. Right: Soft quench, with $r(t>0) = T[1-(t/t_*)e\exp(-t/t_*)]$, $t_*T = 30$.

HARD QUENCH

Electron Andreev reflects into a hole. This process is resonant for electrons at the Fermi energy.

Lifetime

Universal

Can we see this in observables?

$$Im\Sigma \equiv \tau^{-1} = t^{\frac{3-d}{2}} g_d(\xi^2 T t)$$

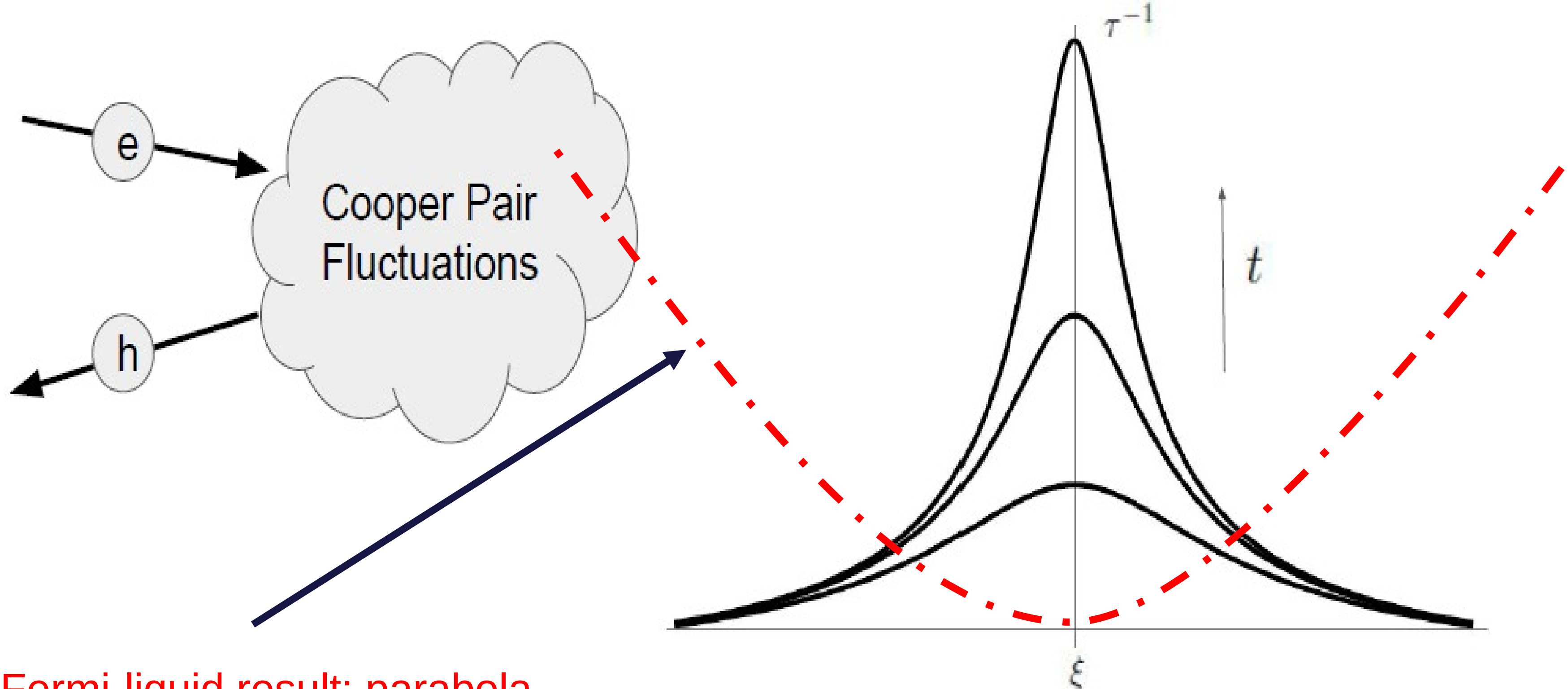

Fermi-liquid result: parabola

Non-Fermi liquid as life-time is shorter at the Fermi-energy.

Conductivity of transient state

$$J(t) = \int dt' \sigma(t,t') E(t'),$$

Optical conductivity $\sigma(\omega,t) = \int d\tau\, \sigma(t+\tau,t) \exp(i\omega\tau)$

Galilean invariant system: Momentum is proportional to velocity.
Since momentum is conserved, current never decays

$$\sigma(t,t') \propto \theta(t-t')$$

Broken Galilean invariance: Momentum and velocity no longer proportional. This implies a component of the current will decay.
(We neglect Umklapp processes)

In diagrammatic language:

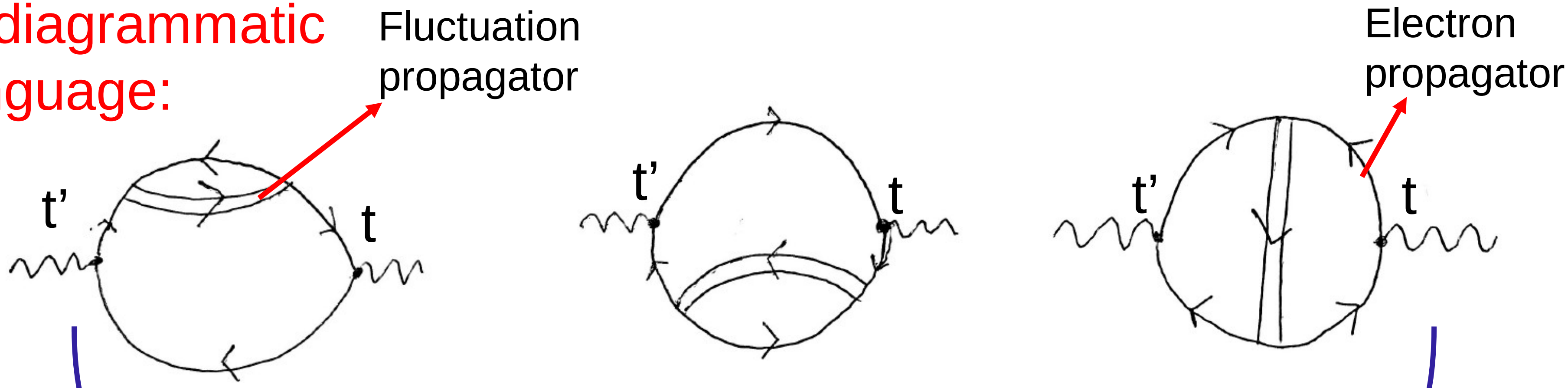

$$\partial_t J(t) - \frac{\rho}{\bar{m}} E(t) = -\frac{1}{\tau_r}\Bigg(A(t) J(t) - \alpha \int_0^t dt' \Big[B(t,t') J(t') + \frac{\rho}{2\bar{m}} C(t,t') E(t') \Big] \Bigg)$$

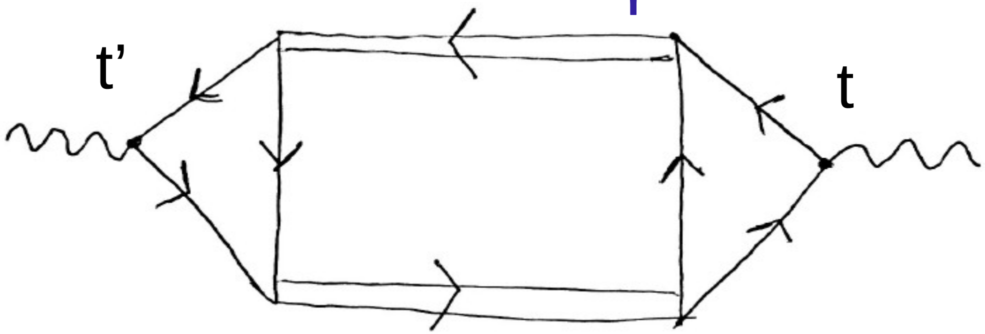

Azlamazov-Larkin diagram

Conductivity for the hard quench. $r = 0$

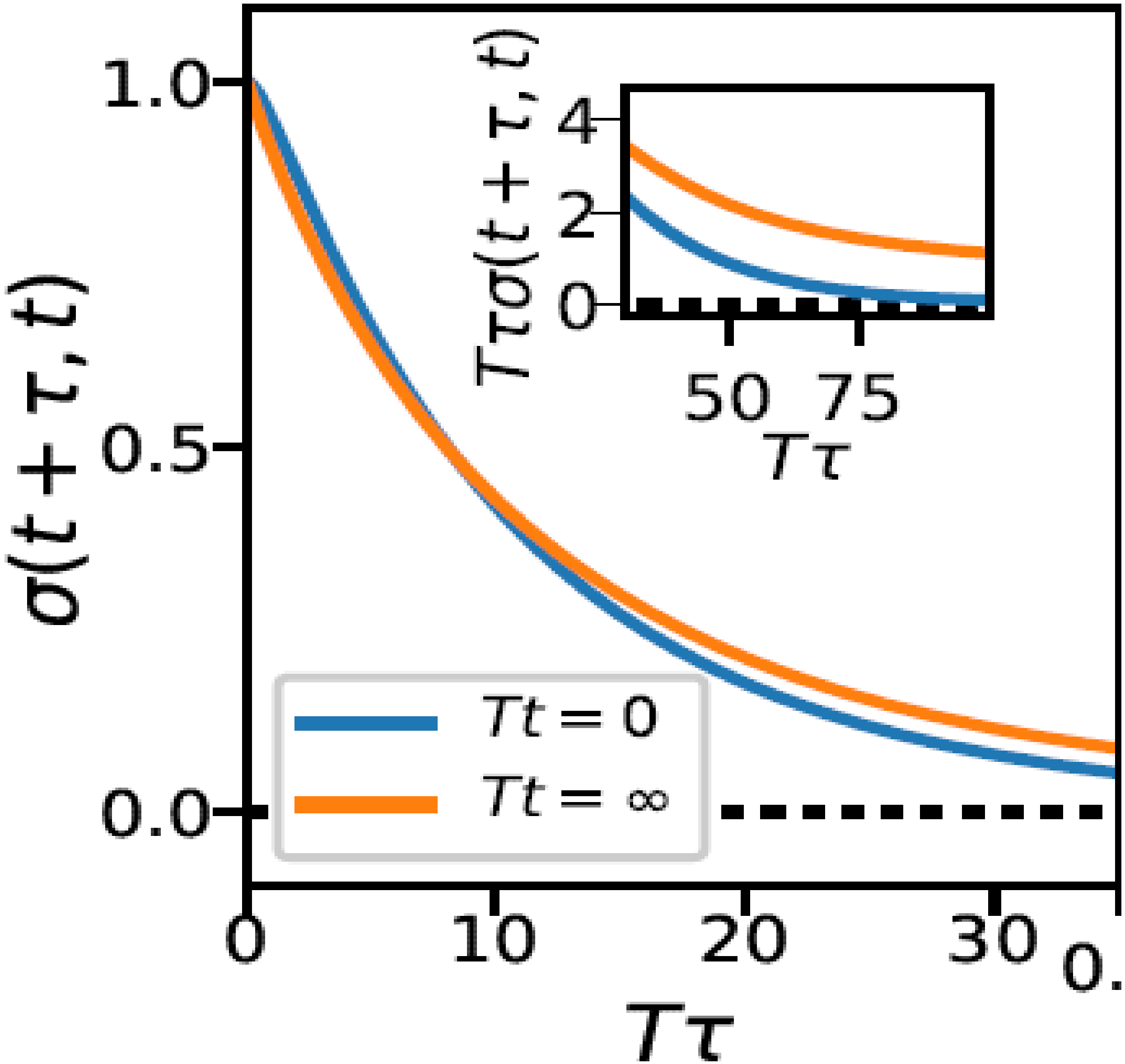

$J(\tau) = \sigma(t+\tau, t)$,
$E(t) = \delta(t)$

t=Delay time between quench and probe

$T\tau_r = 5,\ \alpha = 0.5$

In the inset are the tails of $\sigma(t+\tau,t)$, $T\tau > 30$, plotted as $T\tau\sigma(t+\tau,t)$ to improve visibility.

Time-evolution of the optical conductivity, for a critical quench

$$\sigma(\omega, t) = \int d\tau \, \sigma(t+\tau, t) \exp(i\omega\tau)$$

Low-frequency conductivity changes as log(t). Saturation at Log[min(frequency,1/t)]

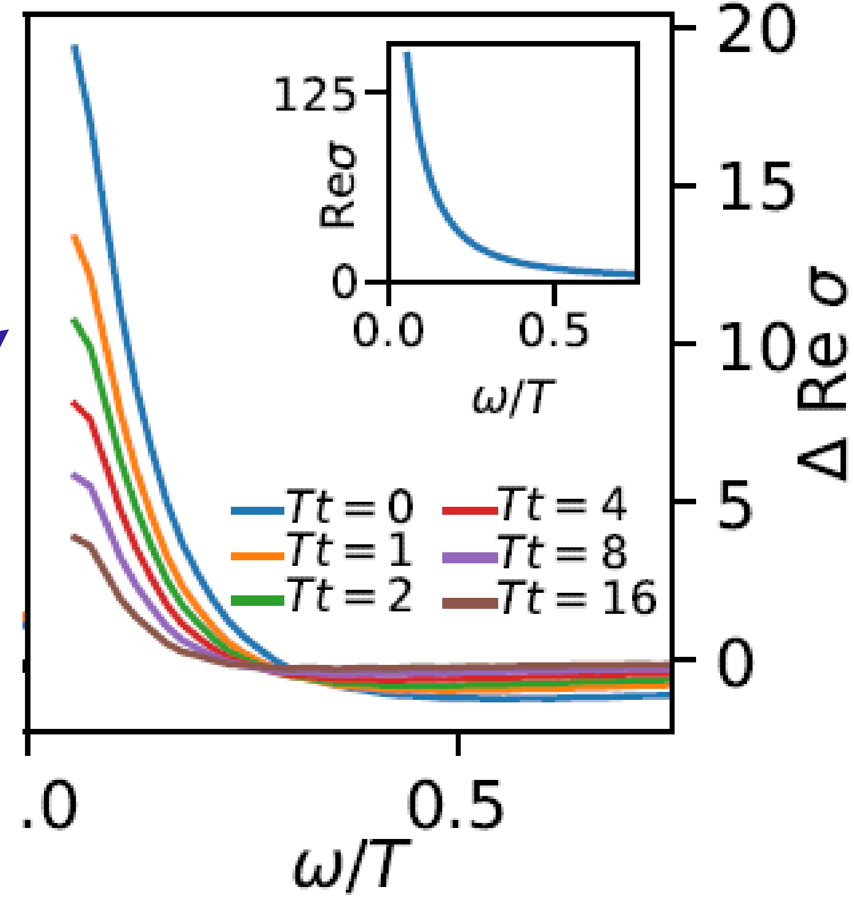

Re $[\sigma(\omega, t) - \sigma(\omega, t \to \infty)]$ for different times since the quench. Note the times increase in a geometric fashion. Inset: Re$\sigma(\omega, t \to \infty)$. This diverges as $\log \omega$ as $\omega \to 0$ so all curves are clipped at $\omega = .01T$

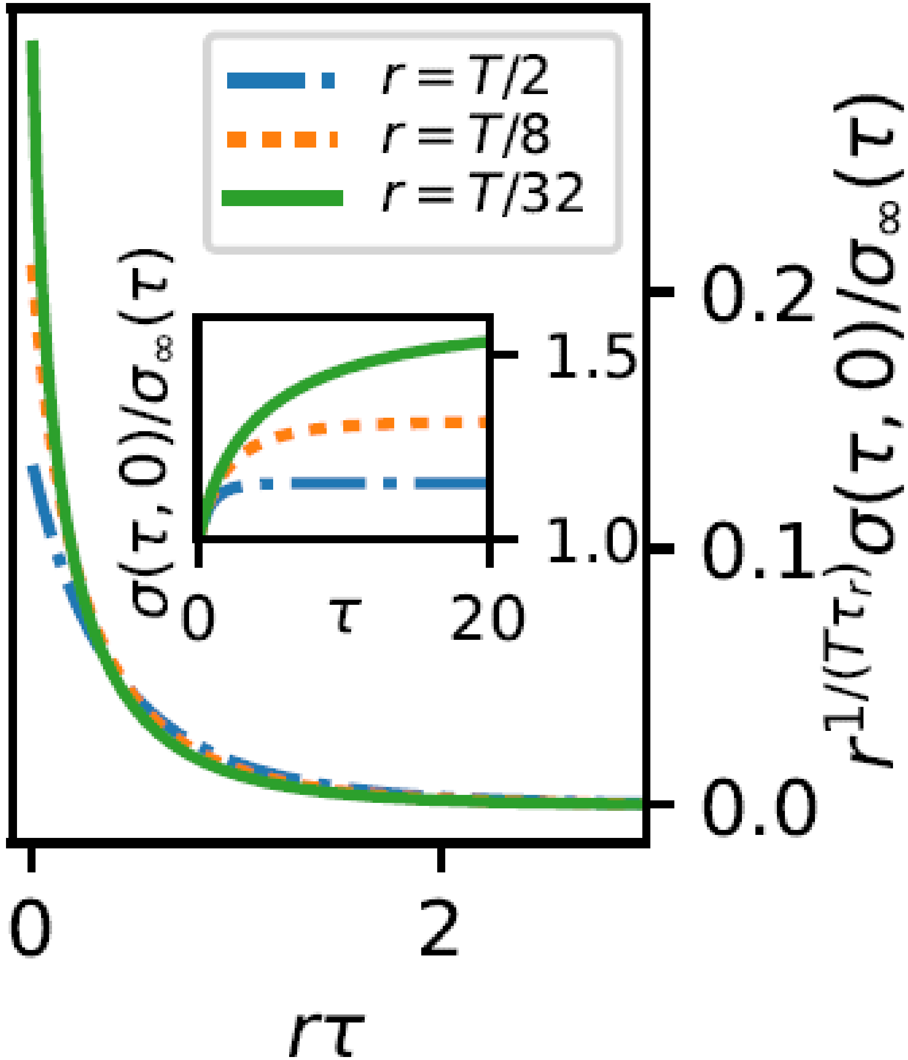

Scaling plot of the $\sigma(\tau, 0)$ at $\alpha = 0$ for different detunings r. Inset: unscaled $\sigma(\tau, 0)$. Plots shown for $T\tau_r = 5$.

Optical conductivity for the soft quench

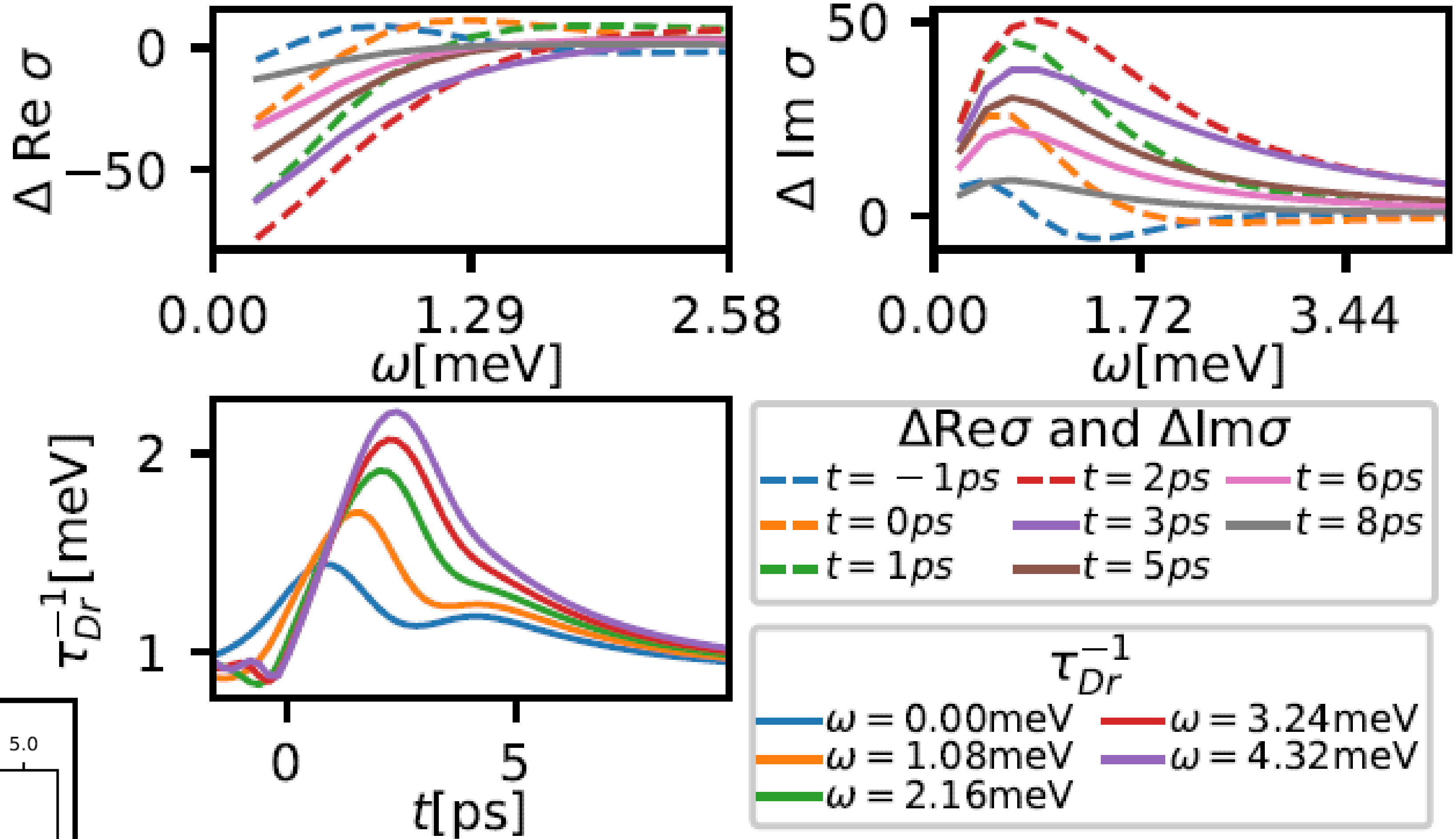

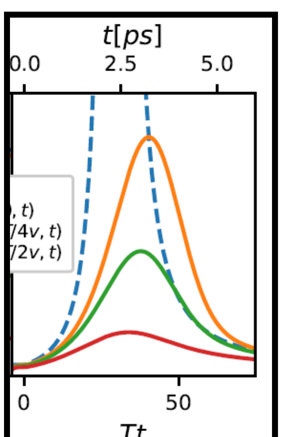

Drude scattering time defined as:

$$\tau_{\mathrm{Dr}}(\omega) = \mathrm{Im}\left[\sigma\right] / \left[\omega \mathrm{Re}\sigma\right]$$

1. Real systems have disorder.

2. Fluctuation conductivity for a strongly disordered metal is well studied. Kubo formalism (linear response) for the optical conductivity is used.

A. I. Larkin and A. A. Varlamov, in *Handbook on Superconductivity: Conventional and Unconventional Superconductors*, edited by K.-H.Bennemann and J. Ketterson (Springer, 2002).

We generalize these studies to a quantum quench.

Disorder

$$H = \sum_{kk's} \Big[(\varepsilon_k \delta_{kk'} + V_{k-k'})\, c^{\dagger}_{ks} c_{k's}$$

$$+ U(t) \sum_{qs'} c^{\dagger}_{ks} c_{k-qs} c^{\dagger}_{k'-qs'} c_{k's'} \Big].$$

$$\langle V_q V_{-q'} \rangle \;=\; \delta_{qq'} / 2\pi\nu\tau$$

As before:
Electrons assumed to thermalize rapidly at temperature T,
Fluctuation propagators are slow due to proximity to critical point.

We also assume strong disorder: $T\tau/\hbar \ll 1$
(many scatterings within a de-Broglie wave-length)

Conductivity = Drude formula + fluctuation correction

$$\sigma = \frac{ne^2\tau}{m} + \ldots\ldots\ldots$$

Azlamazov-Larkin

Maki-Thompson

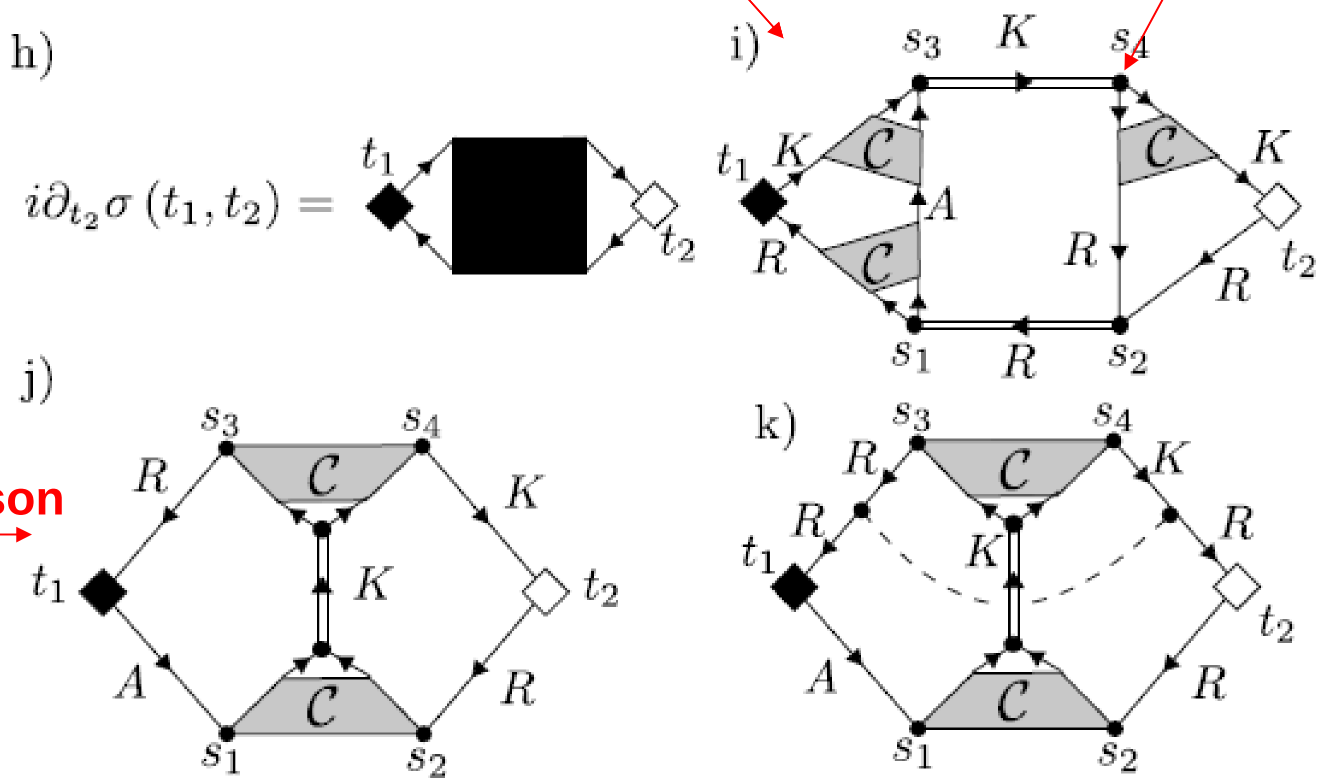

Conductivity in Equilibrium (d=2)

ϵ Detuning from critical point $\qquad \bar{\omega} \equiv \frac{\pi\omega}{16T}$

$$\sigma^{MT}(\bar{\omega}) + \sigma^{AL}(\bar{\omega}) = \frac{1}{16\epsilon}\begin{cases} \frac{4\epsilon}{-i\bar{\omega}}\log\frac{-i\bar{\omega}}{\epsilon} & \bar{\omega} \gg \epsilon, \gamma_\phi \\ 1 - 2\log\frac{-i\bar{\omega}}{\epsilon} & \epsilon \gg \bar{\omega} \gg \gamma_\phi \\ \frac{2\epsilon}{-i\bar{\omega}}\log\frac{-i\bar{\omega}}{\epsilon} + \frac{2\epsilon}{\gamma_\phi}\log\frac{\gamma_\phi}{\epsilon} & \gamma_\phi \gg \bar{\omega} \gg \epsilon \\ 1 + 2\frac{\epsilon}{\gamma_\phi - \epsilon}\log\frac{\gamma_\phi}{\epsilon} & \epsilon, \gamma_\phi \gg \bar{\omega} \end{cases}$$

A. I. Larkin and A. A. Varlamov, in *Handbook on Superconductivity: Conventional and Unconventional Superconductors*, edited by K.-H.Bennemann and J. Ketterson (Springer, 2002).

ϵ Detuning from critical point
B=F = Superconducting fluctuations

Time-evolution of superconducting fluctuations →

$$\left[\frac{\partial}{\partial t} + \frac{16T}{\pi}\left(\epsilon(t) + \xi^2 q^2\right)\right] B_q(t) = T.$$

$$\sigma^{AL}(t_1, t_2) = 32 \int_{-\infty}^{t_2} ds \int \frac{d^2q}{(2\pi)^2} \xi^4 q^2 \nu^2 |D_R(q, t_1, s)|^2 B_q(s) \quad (11a)$$

$$\sigma^{MT}(t_1, t_2) = 16D \int \frac{d^2q}{(2\pi)^2} B_q\left(\frac{t_1 + t_2}{2}\right) e^{-2\left(\frac{1}{\tau_\phi} + Dq^2\right)(t_1 - t_2)} \quad (11b)$$

τ_ϕ : Phase coherence time

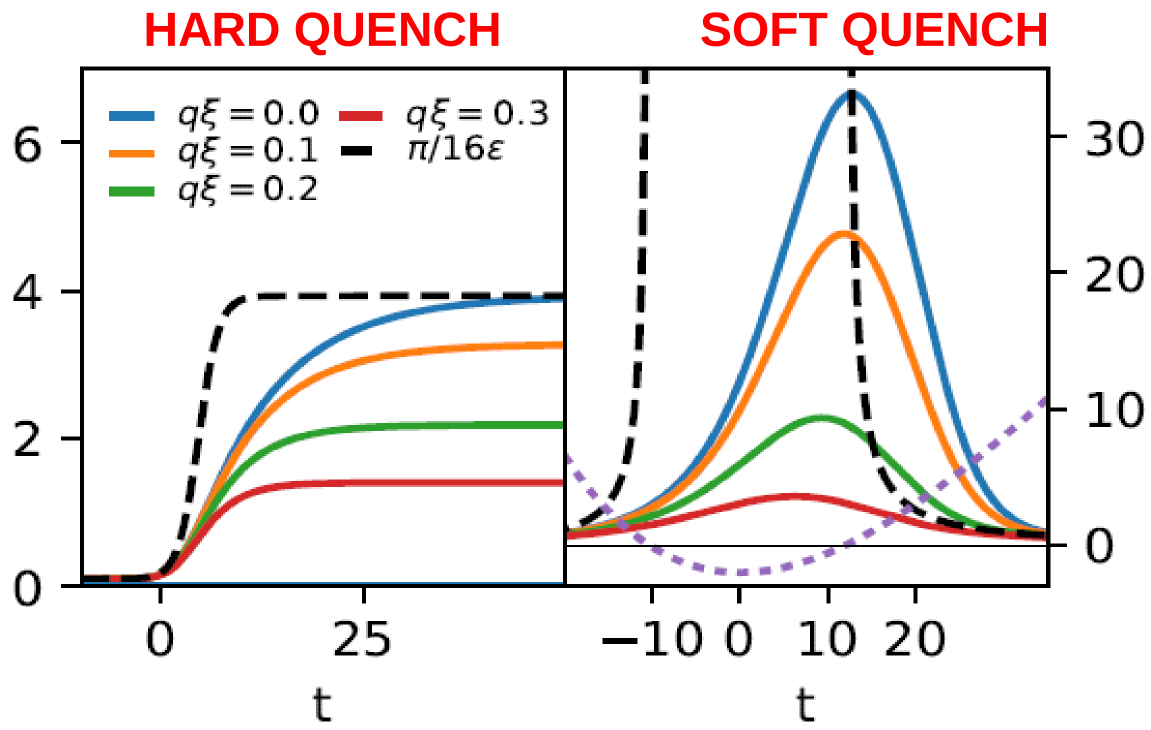

FIG. 1. The growth of the superconducting fluctuation at different lengths (q^{-1}) under a changing detuning $\epsilon(t)$ from the superconducting critical point. The time is given in units of $\pi\hbar/8T$. The dashed line shows $\pi/16\epsilon(t)$ which equals $B(q = 0)$ in equilibrium. The dotted purple line in the right panel gives $\epsilon(t)$ at arbitrary scale. In the left panel the detuning saturates at the value $\epsilon = 0.05$. In the right panel, the detuning is $\epsilon(t) = \epsilon_0 + (\epsilon_{\min} - \epsilon_0)(t/t_* e)\exp(-t/t_*)\theta(t)$ with the parameters $t_* = 30$, $\epsilon_0 = 1$, $\epsilon_{\min} = -0.05$.

coherence length $\xi = \sqrt{\pi D/8T}$

$D = v_F^2\tau/d$ is the diffusion constant

AGING FOR A CRITICAL QUENCH:

Azlamazov-Larkin

$$\sigma(t_1, t_2) = \frac{2T}{\pi}\Big[-\frac{t_2}{t_1} - \log\left(1 - \frac{t_2}{t_1}\right) + e^{-2(t_1-t_2)/\tau_\phi} \log\left(1 + \frac{1}{2}\frac{t_1+t_2}{t_1-t_2}\right)\Big],$$

Maki-Thompson

Experimentally determine the phase-breaking time?

HARD QUENCH

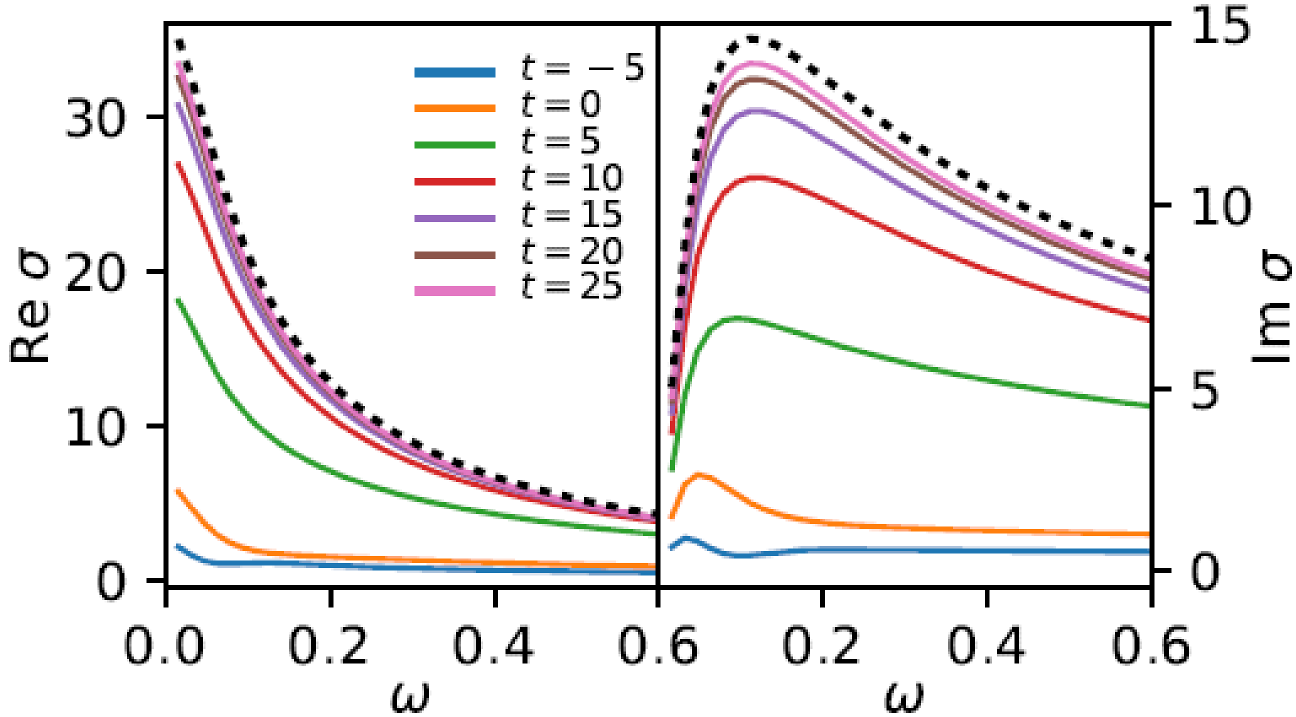

FIG. 3. Conductivity $[e^2/\hbar]$ as a function of frequency for several times. The left panel shows real part, the right panel shows the imaginary part. All times are in units of $\pi\hbar/8T$. The detuning ϵ varies according to Fig. 1, left panel and $\tau_\phi = 20 \times (\hbar\pi/8T)$. The dashed line gives the equilibrium result for the final value of the detuning $\epsilon = .05$.

SOFT QUENCH

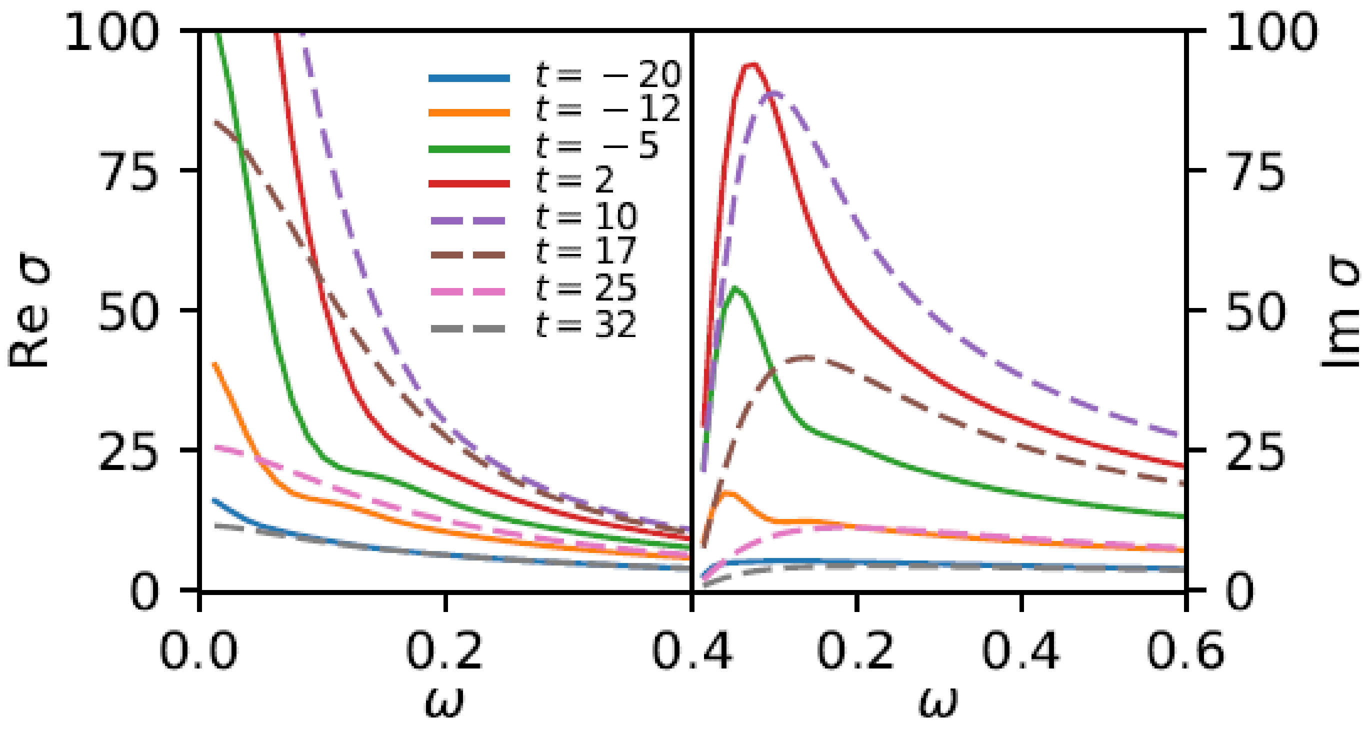

FIG. 4. Conductivity $[e^2/\hbar]$ as a function of frequency for several times, all in units of $\pi\hbar/8T$. The detuning is given in Fig. 1, right panel and $\tau_\phi = 20 \times (\hbar\pi/8T)$. In order to improve clarity, lines for $t \leq 2$ are shown with full lines and those for $t > 2$ are shown with dashed lines. The conductivity σ as $\omega \to 0$ reaches a maximum of ~ 175 at $t \approx 7$.

Initially free system of electrons. Quench involves turning on attractive BCS interactions.

Many competing superconducting order-parameters in realistic systems. By tuning the quench amplitude, order parameters of different symmetries can be realized.

Graphene irradiated with circularly polarized laser

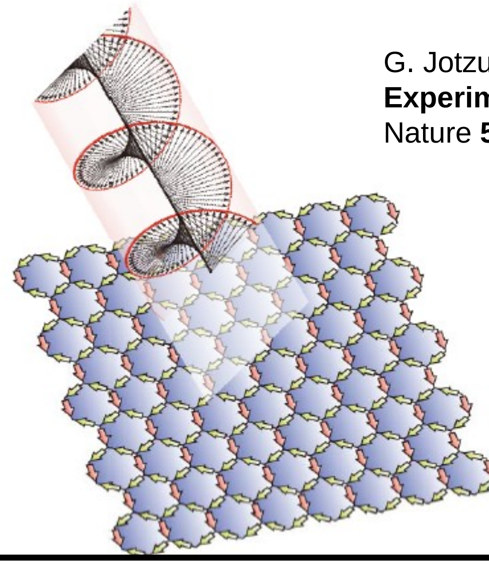

G. Jotzu, T. Esslinger et al.:
Experimental realization of the topological Haldane model
Nature **515**, 237-240 (2014).

Oka and Aoki PRB 2009 in graphene
Other models:
Kitagawa et al PRB 2011,
Lindner et al Nature 2011
Yao, MacDonald, Niu et al PRL 2007

$$U(T+t,t)=e^{-iH_{eff}T}$$

$$H_{eff}\approx k_x\sigma_x\tau_z+k_y\sigma_y+\frac{A_0^2}{\Omega}\sigma_z\tau_z$$

σ:Sublattice index

τ :K,K' points

Breaks time-reversal

H_{eff} **Maps onto the Haldane model**

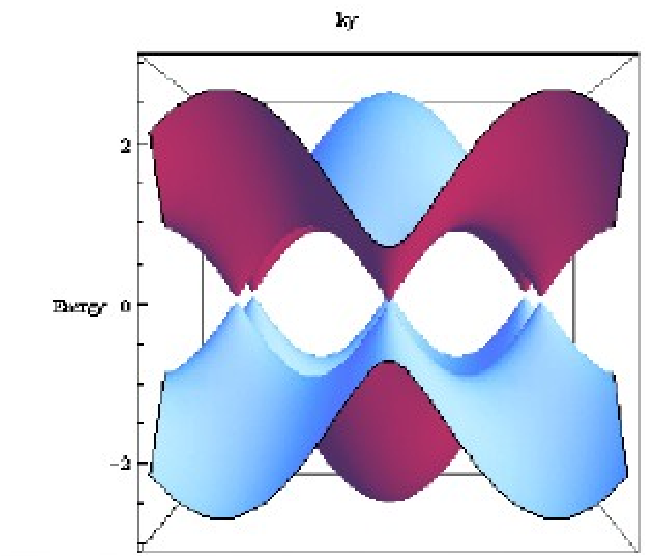

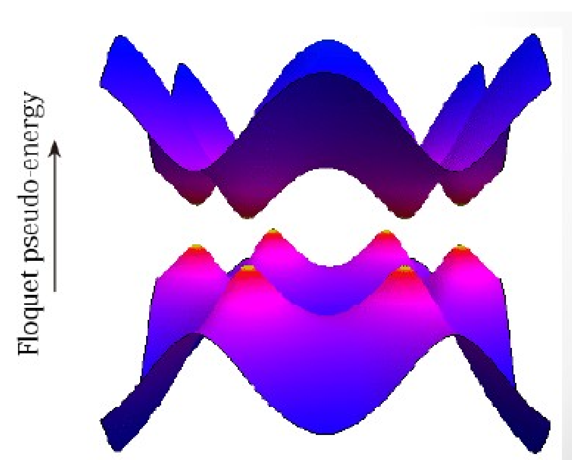

Initial Hamiltonian Heff: Graphene and/or Haldane model

Final Hamiltonian H: Attractive BCS interactions

$$V = J \sum_{<ij>} \left[\vec{S}_i \cdot \vec{S}_j - \frac{1}{4} n_i n_j \right]$$

$$\Delta_\alpha = J \left\langle b_{i+\alpha\downarrow} a_{i\uparrow} - b_{i+\alpha\uparrow} a_{i\downarrow} \right\rangle$$

$\alpha = 1, 2, 3$ denote the three nearest neighbor bonds

$$H = H_{\mathrm{eff}} - \sum_{k,\alpha} \left[\Delta_\alpha e^{i\vec{k}\cdot\vec{a}_\alpha} \left(a^\dagger_{k\uparrow} b^\dagger_{-k\downarrow} - a^\dagger_{k\downarrow} b^\dagger_{-k\uparrow} \right) + h.c. \right].$$

We will monitor how an initial superconducting fluctuation evolves in time.

$$\Delta_\alpha(t) = J \sum_\beta \int_0^t dt' \Pi^R_{\alpha\beta}(q = 0, t, t') \Delta_\beta(t').$$

SC in doped graphene in equilibrium

R. Nandkishore, L. Levitov, and A. Chubukov, Nature Physics **8**, 158 (2012).
A. Black-Schaffer and C. Honerkamp, Journal of Physics Condensed Matter **26** (2014).

$$\Delta_s = \frac{1}{\sqrt{3}}[1,1,1]$$

$$\Delta_{d+id} = \frac{1}{\sqrt{3}}\begin{pmatrix}1\\ e^{2\pi i/3}\\ e^{4\pi i/3}\end{pmatrix}$$

$$\Delta_{d-id} = \frac{1}{\sqrt{3}}\begin{pmatrix}1\\ e^{4\pi i/3}\\ e^{2\pi i/3}\end{pmatrix}$$

Graphene: C3 symmetry and time-reversal symmetry

$$\Pi^R(t) = \begin{pmatrix} A(t) & B(t) & B(t)\\ B(t) & A(t) & B(t)\\ B(t) & B(t) & A(t)\end{pmatrix}.$$

Eigenvalues (EV): s-wave. And two degenerate EV: d+id and d-id

Haldane model: C3 symmetry but broken time-reversal symmetry

$$\Pi^R(t) = \begin{pmatrix} A(t) & B(t) & C(t)\\ C(t) & A(t) & B(t)\\ B(t) & C(t) & A(t)\end{pmatrix}.$$

3 Non-degenerate eigenvalues: s-wave, d+id and d-id.

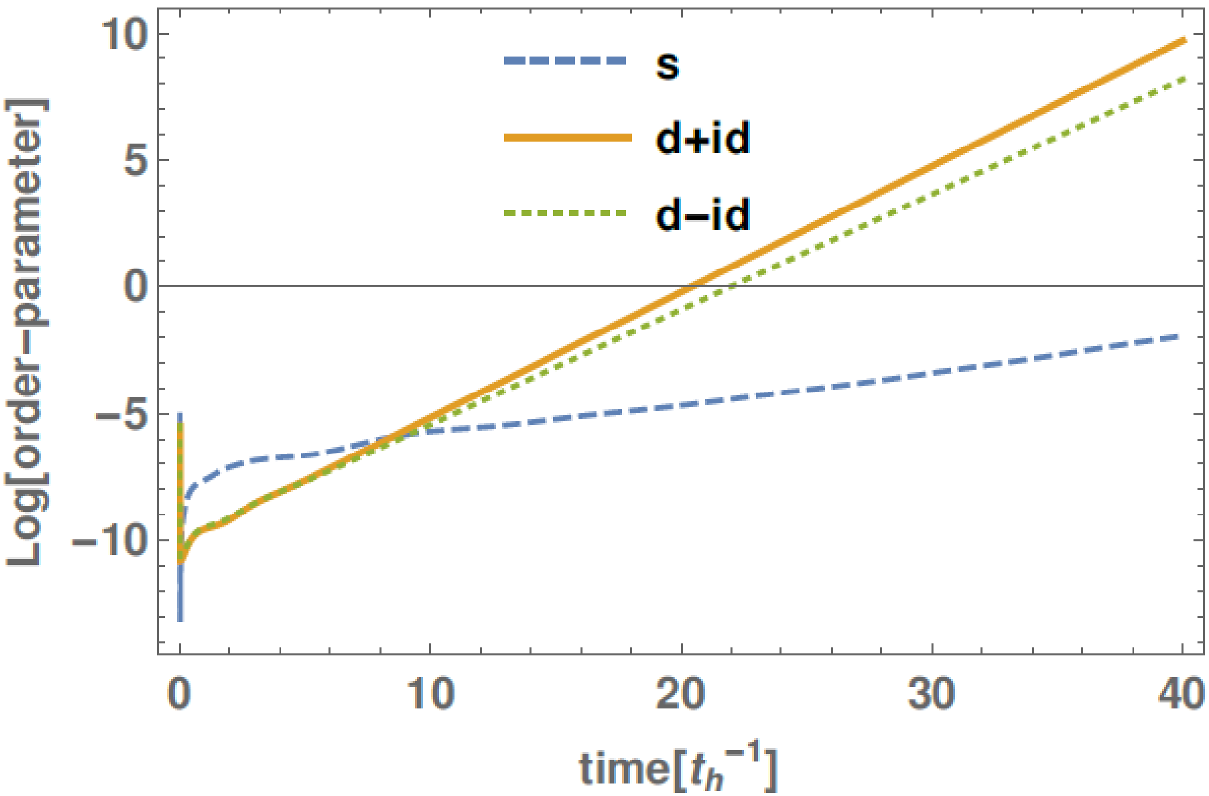

FIG. 1: Haldane model
$A_0 a = 0.5, \Omega = 10t_h, J = 1.82t_h, T = 0.01t_h$ and doping $\delta = 0.1$. Time-evolution of the logarithm of an initial random vector. The time-evolution is projected along the three orthogonal directions with s, $d + id$, $d - id$ symmetry. The slopes indicate that for the chosen parameters $d + id$ is the fastest growing instability, followed by $d - id$ and then s. Time is in units of t_h^{-1}.

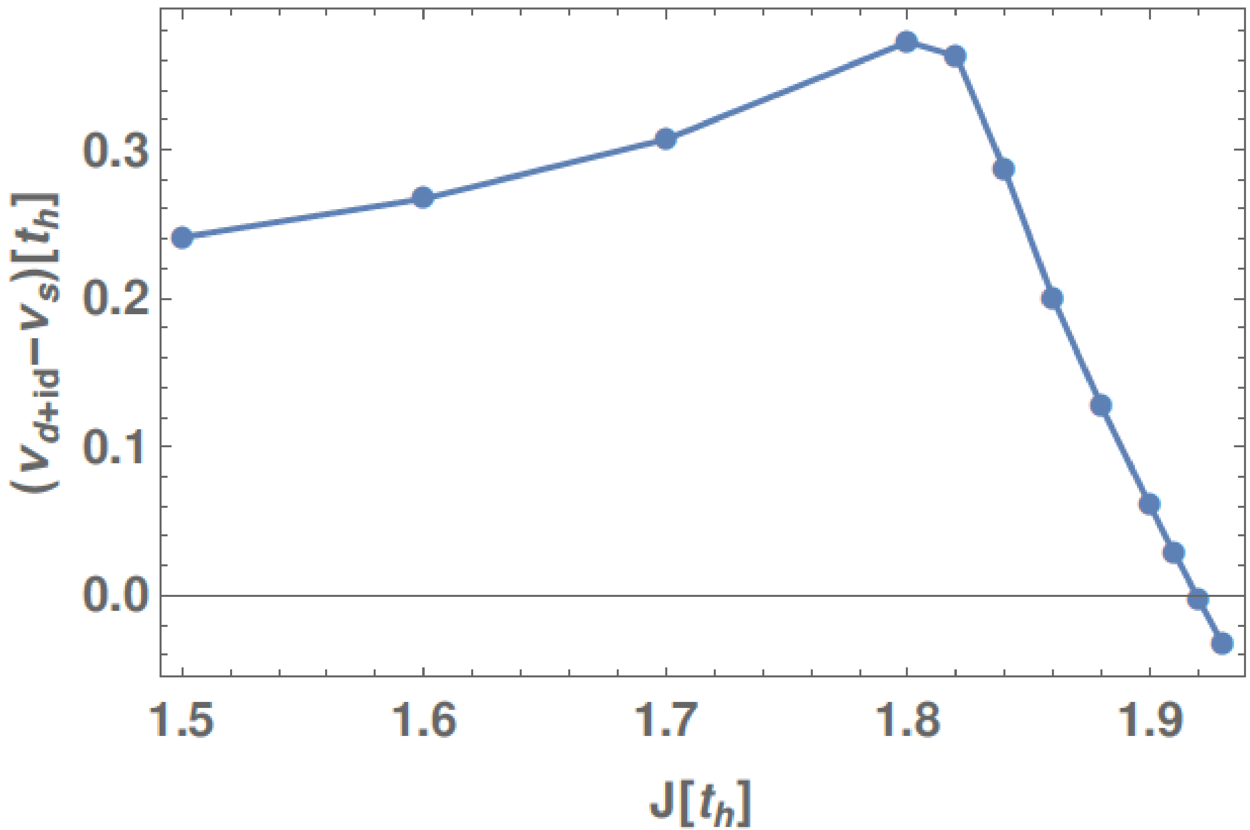

FIG. 2: Haldane model $A_0 a = 0.5, \Omega = 10t_h, T = 0.01t_h$ and doping $\delta = 0.1$ (same as Fig. 1). As the quench amplitude J is increased, the difference between the growth rate of chiral d-wave (ν_{d+id}) and s-wave (ν_s) varies as shown above. The difference first increases, and then decreases rapidly. For quench amplitudes larger than $J_c \sim 1.9$ the s-wave is preferred.

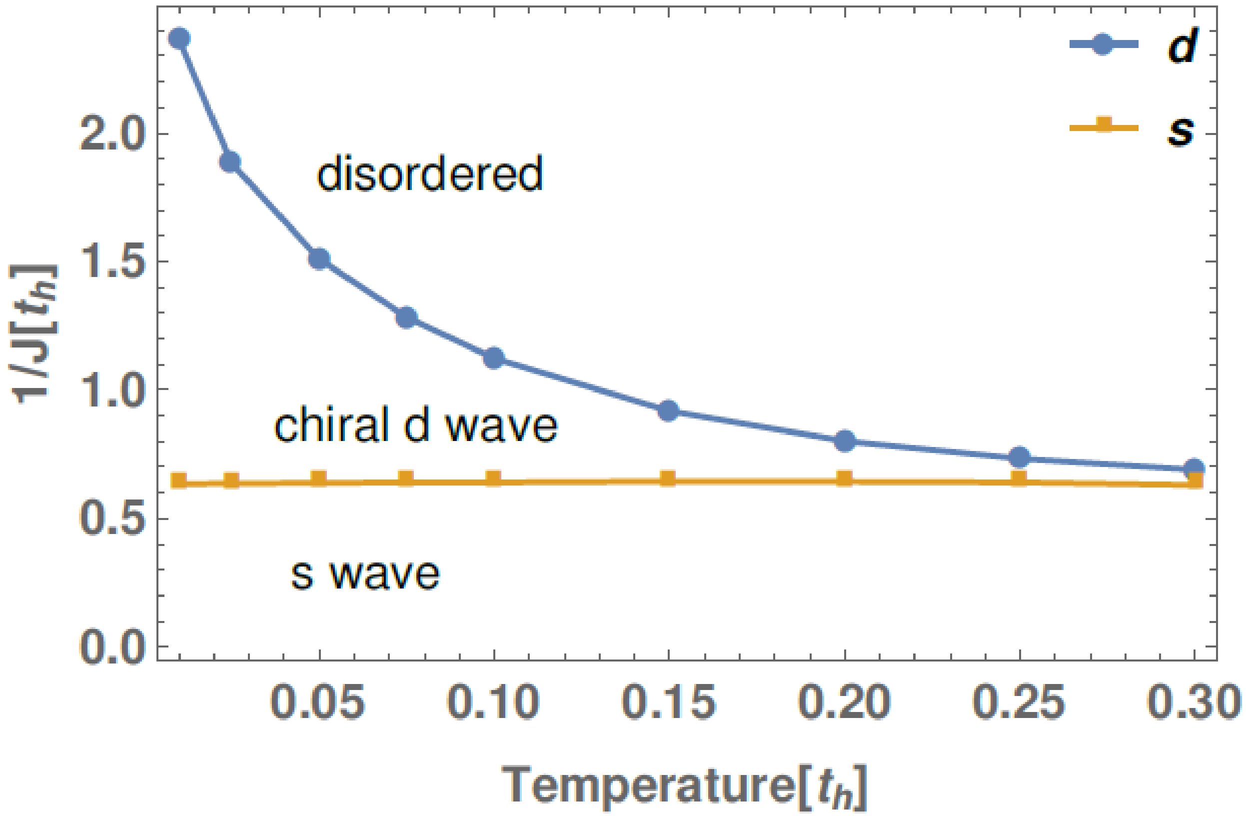

FIG. 5: Haldane model $A_0a = 1.0, \Omega = 10t_h$ and doping $\delta = 0.1$. The phase diagram determined by the fastest growing order parameter. The line corresponding to the transition from the disordered (normal) phase to the chiral d-wave phase coincides with the equilibrium phase diagram. As the quench amplitude is increased, the s-wave phase is preferred.

Dephasing effects due to excited quasi-particles detrimental for d-wave pairing

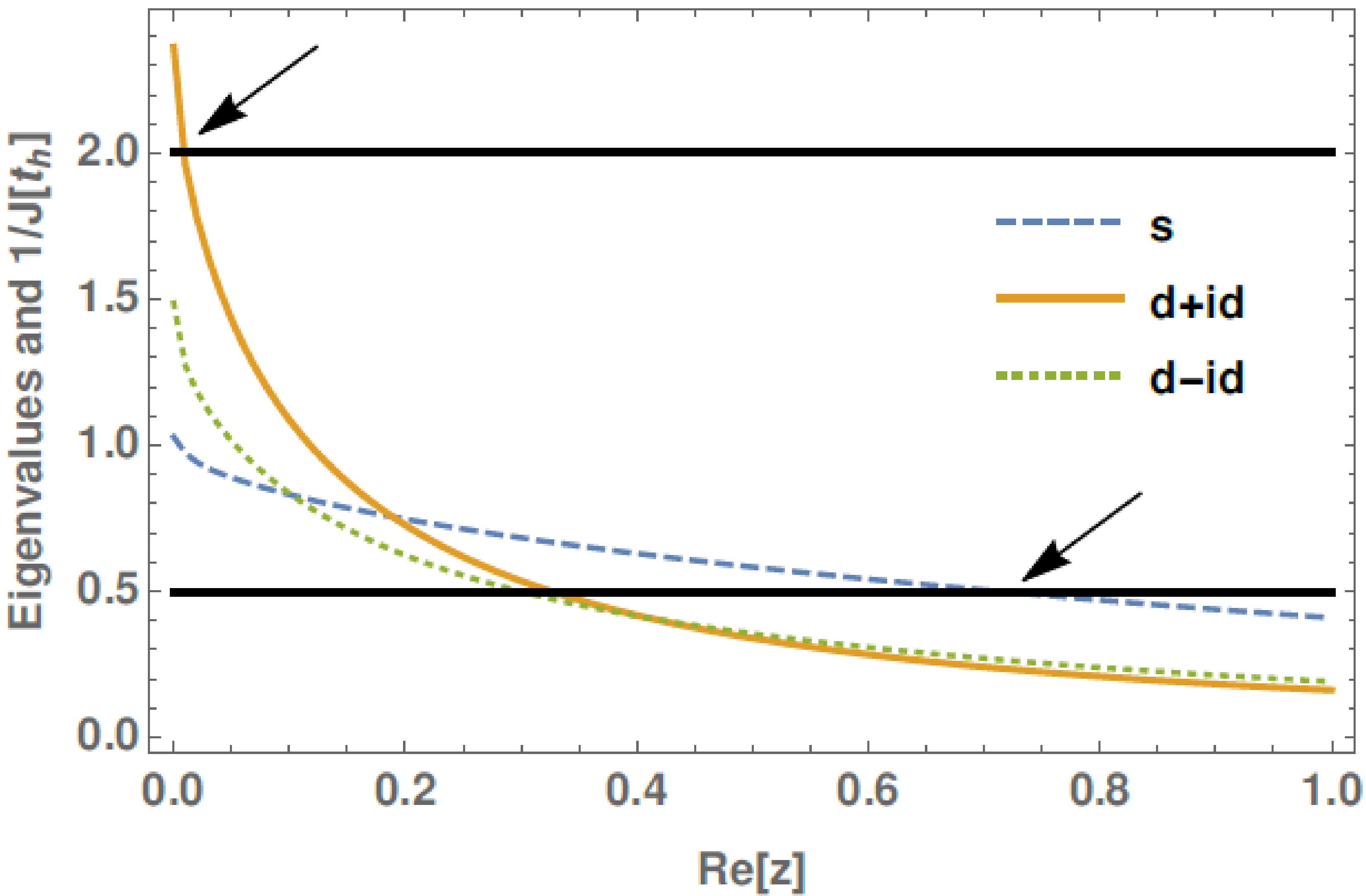

Eigenvalues and 1/J[t_h]
2.0
1.5
1.0
0.5
0.0
0.0
0.2
0.4
0.6
0.8
1.0
Re[z]
s
d+id
d−id

Conclusions:

1. Pump-probe spectroscopy of correlated materials, and near unitary dynamics of cold-atomic gases, has opened up exciting new regimes of non-equilibrium physics of interacting systems.
2. Results were presented for an interacting electron gas that traverses arbitrarily close to a superconducting critical point. Even though the system is not ordered in the conventional sense, time-dependent behavior is strongly influenced by superconducting fluctuations.
3. Time resolved optical conductivity and time resolved ARPES show clear features of approaching a superconducting critical point.
4. Strongly disordered case reveals power-law scaling of the conductivity for critical quenches whose functional form depends on the relative importance of Azlamazov-Larkin and Maki-Thompson terms.
5. An example was also presented of how the symmetries of a superconducting order parameter may be influenced by the interaction quench amplitude.